ISSN 0021-3640, JETP Letters, 2009, Vol. 89, No. 12, pp. 621–625. © Pleiades Publishing, Ltd., 2009.
Original Russian Text © V.S. Zhigalov, V.G. Myagkov, O.A. Bayukov, L.E. Bykova, G.N. Bondarenko, A.A. Matsynin, 2009, published in Pis'ma v Zhurnal Éksperimental'noĭ i Teoreticheskoĭ Fiziki, 2009, Vol. 89, No. 12, pp. 725–729.

Phase Transformations in Mn/Fe(001) Films: Structural and Magnetic Investigations

V. S. Zhigalov[a], V. G. Myagkov[b], O. A. Bayukov[b], L. E. Bykova[b], G. N. Bondarenko[c], and A. A. Matsynin[a]

[a] *Reshetnev Siberian State Aerospace University, Akademgorodok, Krasnoyarsk, 660036 Russia*
e-mail: zhigalov@iph.krasn.ru

[b] *Kirensky Institute of Physics, Siberian Branch, Russian Academy of Sciences, Akademgorodok, Krasnoyarsk, 660036 Russia*

[c] *Institute of Chemistry and Chemical Technology, Siberian Branch, Russian Academy of Sciences, Krasnoyarsk, 660036 Russia*

Received April 9, 2009; in final form, May 13, 2009

The solid-phase synthesis in epitaxial Mn/Fe(001) bilayer film systems with 24 at % of Mn has been shown to start at a temperature of 220°C with the formation of a γ-austenite lattice and the Mn and Fe films react completely under annealing to 600°C. In the sample cooling process after annealing below 220°C, the γ austenite undergoes a martensitic transformation to an oriented ϵ(100) martensite. When the annealing temperature is increased above 600°C, Mn atoms migrate from the γ-lattice, which becomes unstable, and the film is partially again transformed to the epitaxial Fe(001) layer. The solid-phase synthesis in Mn/Fe(001) bilayer nanofilms and multilayers is assumingly determined by the inverse $\epsilon \longrightarrow \gamma$ martensitic transformation in the Mn–Fe system. The existence of a new low-temperature (~220°C) structure transition in the Mn–Fe system with a high iron content is assumed.

PACS numbers: 66.30.Pa, 81.15.Np, 81.20.Ka, 81.30.Bx

DOI: 10.1134/S0021364009120066

INTRODUCTION

Experimental and theoretical investigations show that Mn layers on metal surfaces have unusual structure and magnetic properties [1, 2]. It is well known that α-Mn has a complex cubic structure, whereas high-temperature γ- and δ-Mn phases have simple fcc and bcc lattices, respectively. This implies the stabilization of high-temperature phases by the epitaxial growth of thin Mn films on a cubic (001) substrate [3]. The deposition of Mn on the Fe(001) surface leads to the formation of a deformed body-centered tetragonal structure [4, 5]. Mössbauer data indicate the presence of the Fe_xMn_{1-x} alloy at the interface in the Mn/Fe samples, which grows at temperatures above 50°C [5]. The photoemission measurements indicate mixing at the Mn/Fe interface at 150°C [6]. The alloying of ultrathin Mn films with FeNi is observed after 20-s annealing at 280°C [7]. The synthesis of the ϵ and γ phases of the Mn–Fe system was performed in Mn/Fe bilayer films subjected to irradiation by krypton ions [8] and to mechanical alloying [9]. The conditions of the solid-phase alloying Mn with Fe and the formation of Fe_xMn_{1-x} alloys remain unstudied. These melts with a high iron content have unique properties including low-temperature (~200°C) martensitic transformations [10] and the invar effect [11] and are used as antiferromagnetic layers in film structures with exchange interaction [12].

In this work, the solid-phase transformations of a polycrystalline Mn film deposited on an epitaxial Fe(001) layer are investigated. The results show that the oriented ϵ(100) martensite is formed in the reaction products in a temperature range of 220–600°C. At annealing temperatures above 600°C, Mn is desorbed from the film and the initial Fe(001) layer is recovered.

SAMPLES AND THE EXPERIMENTAL PROCEDURE

Mn/Fe(001) film structures were manufactured using the thermal evaporation method by the electron bombardment of a Mo crucible in a vacuum of 10^{-6} Torr. The first Fe layer with a thickness of 150 nm was deposited on a single-crystal MgO(001) substrate at a temperature of 220–250°C. At these temperatures, α-Fe crystallites grow epitaxially by the (001) plane on the MgO(001) surface. The subsequent Mn layer 40–50 nm in thickness was deposited at room temperature in order to avoid an uncontrolled reaction with the Fe layer. The thin upper Fe layer with a thickness of about 10 nm was deposited in order to protect the Mn film against oxidation. At these relations

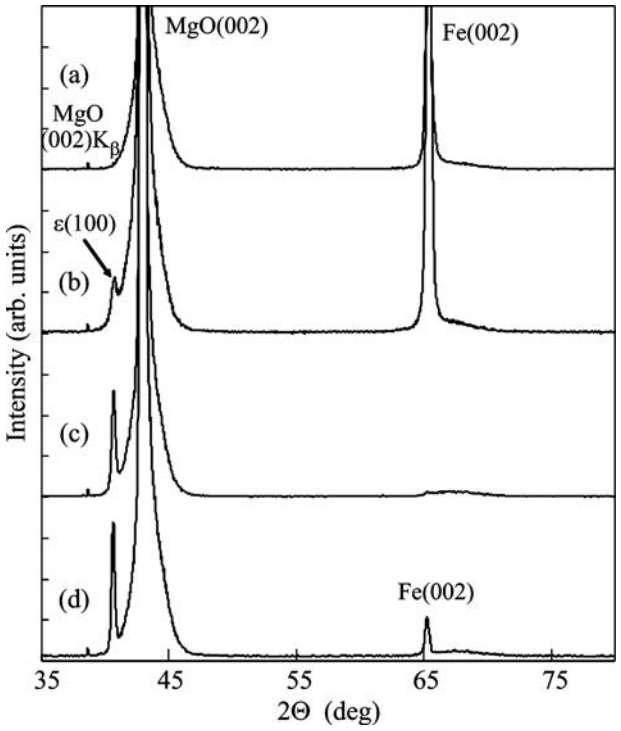

Fig. 1. X-ray diffraction patterns of the epitaxial Mn/Fe(001) film system after annealing at temperatures of (a) 20, (b) 250, (c) 600, and (d) 800°C.

between the thicknesses, the resulting samples correspond to a nominal Mn content of about 24 at %. The Mn_xFe_{1-x} melts with these contents exhibit an $\epsilon \longleftrightarrow \gamma$ martensitic transformation. The initial film samples were annealed in a vacuum in a temperature range of 100 to 800°C with a step of 50°C for 30 min at each temperature. The saturation magnetization M_S and

Mössbauer parameters of the films after annealing at various temperatures: isomeric chemical shift (*IS*) with respect to α-Fe, hyperfine field *H*, quadrupole splitting Q_S, line width *W*, and occupation of nonequivalent sites *A*

	IS, mm/s	*H*, kOe	Q_S, mm/s	*W*, mm/s	*A*, %
20°C	0.008	331	0	0.30	95
	0.129	212	0.01	0.18	5
200°C	–0.089	0	0.61	0.42	77
	–0.082	0	0	0.40	23
800°C	0.015	336	0	0.24	10
	0.010	325	0	0.29	23
	0	309	0	0.40	29
	–0.015	299	–0.06	0.19	6
	–0.020	281	0.04	0.64	24
	–0.090	0	0	0.28	8

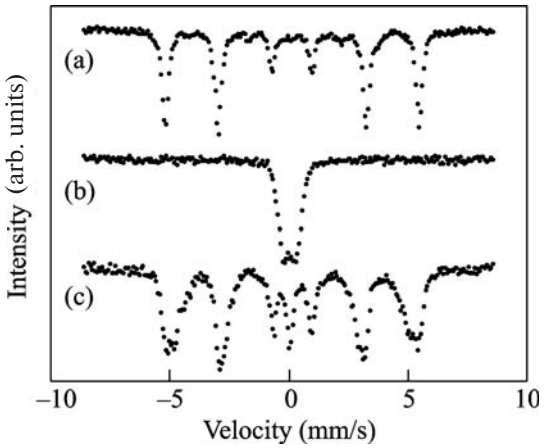

Fig. 2. ^{57}Fe Mössbauer spectra of the epitaxial Mn/Fe(001) film system after annealing at temperatures of (a) 20, (b) 600, and (c) 800°C.

first crystallographic anisotropy constant K_1 were measured using the torsion torque method with a maximum magnetic field of 18 kOe. The Mössbauer spectra were measured with a Co^{57} (Cr) source in a constant acceleration regime. The phase content and structure parameters were obtained by X-ray spectroscopy on a DRON-4 diffractometer. The thicknesses of the Mn and Fe layers were determined by X-ray fluorescence analysis. All of the measurements were performed at room temperature. The electric resistance was measured by the four-probe method.

EXPERIMENTAL RESULTS

The X-ray spectrum of the initial Mn/Fe(001) sample contains only the Fe(002) reflection (see Fig. 1a), which indicates the epitaxial growth of the Fe layer deposited on the MgO(001) surface. Owing to the polycrystalline structure, Mn reflections are absent in the spectrum. The ratio of the areas of the sextet lines in the Mössbauer spectrum of the initial Mn/Fe(001) sample (see Fig. 2a) is 3 : 4 : 1 and the hyperfine structure parameters (see table) are characteristic of the α-Fe layer with a magnetization lying in the film plane. A 5% admixture of the additional phase with a field of 212 kOe is likely attributed to the interlayer iron. The initial Mn/Fe(001) samples had also biaxial anisotropy with the constant equal to the first magnetic crystallographic anisotropy constant K_1 of bulk iron. The analysis of the orientation of easy axes shows that the lower Fe(001) layer grows on MgO(001) according to the orientation relation Fe(001)[110] || MgO(001)[100]. The structure features and magnetic characteristics of the Fe(001) layer deposited on MgO(001) were described in detail in our previous publications [13].

Figure 3 shows the (a) normalized saturation magnetization M_S and (b) normalized magnetic crystallo-

graphic anisotropy constant K_1 as functions of the annealing temperature T_S. Up to a temperature of 200°C, M_S and K_1 remain unchanged, indicating the absence of mixing and the formation of compounds only at the interfaces between the Mn and Fe layers. At annealing temperatures above 200°C, M_S and K_1 decrease and vanish at 600°C. The simultaneous decrease in the saturation magnetization M_S and magnetic anisotropy constant K_1 indicates the formation of nonferromagnetic phases in the reaction products. A further increase in the annealing temperature to 800°C leads to an increase in M_S and K_1 (see Fig. 3).

The measured temperature dependences $M_S(T_S)$ and $K_1(T_S)$ of the Mn/Fe(001) film structure are in agreement with the evolution of the X-ray spectra of these samples (see Fig. 1). The diffraction patterns remain unchanged up to a temperature of 200°C, confirming the absence of the formation of new compounds in the initial Mn/Fe(001)/MgO(001) samples. The sharp decrease in the Fe(002) peak at annealing temperatures above 200°C and the formation of a new reflection with a parameter of 0.222 nm (see Fig. 1b) confirm the start of the solid-phase reaction between the Mn and Fe layers. This peak corresponds to the (100) reflection of the ϵ-martensite, which increases with the annealing temperature (see Fig. 1c). The Mössbauer spectrum confirms the formation of the paramagnetic ϵ-MnFe phase (see Fig. 2b and table), which constitutes the main part (77%) of the material. The remaining part of the alloy (23%) is the γ phase. An increase in the annealing temperature to 600°C leads to the complete disappearance of the Fe(002) reflection (see Fig. 1c). These data completely agree with the magnetic measurements and indicate that the Fe layer completely reacts with the Mn film at 600°C (see Fig. 3). The increase in M_S and K_1 for films annealed in a range of 600 to 800°C (see Fig. 3) is associated with the repeated formation of the epitaxial Fe(001) layer, which is confirmed by the appearance of a strong (002) reflection in the diffraction patterns (see Fig. 1d) and a sextet again appears in the Mössbauer spectrum (see Fig. 2c). The system is multicomponent (see table) due to the diffusion of manganese and the formation of the FeMn alloy with concentration inhomogeneity. A small fraction of the alloy (8%) remains in the γ state. According to the magnetic measurements (see Fig. 3) and Mössbauer data (see table), 40–60% of the initial iron volume are recovered. The X-ray fluorescence analysis indicates that the amount of Mn in the films annealed at 800°C is about halved.

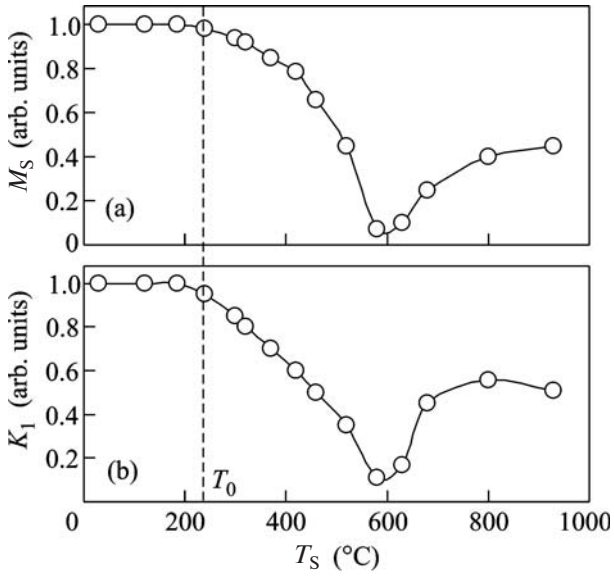

Fig. 3. Annealing temperature dependences of the (a) normalized saturation magnetization M_S and (b) normalized magnetic crystallographic anisotropy constant K_1 of iron for the Mn/Fe(001) film samples. The vertical dashed lines mark the initiation temperature $T_0 \sim 220$°C of the solid-phase reaction.

DISCUSSION OF THE RESULTS

Taking into account that the epitaxial Fe(001) layer of the initial sample completely reacts with the Mn polycrystalline film at 600°C and again appears at higher annealing temperatures, it is assumed that the Fe(001) lattice is only slightly modified during annealings. This allows for the following topotaxial scenario of the development of structure phase transitions in the Mn/Fe(001) samples. The Mn/Fe interface remains sharp up to the initiation temperature $T_0 \sim$ 220°C. As the annealing temperature increases above 220°C up to $T_S \sim 600$°C, Mn atoms migrate along the film normal to the epitaxial Fe(001) layer, partially replacing iron atoms. The formed tetragonal fcc lattice with the parameters $\mathbf{a} = [110]\mathbf{a}_{Fe} = 0.403$ nm and $\mathbf{c} = [100]\mathbf{a}_{Fe} = 0.286$ nm after the Bain deformation is transformed to a γ-austenite lattice with a parameter of 0.354 nm. As the temperature decreases below 220°C, the γ austenite undergoes a martensitic transformation to the ϵ-phase. Such a scenario of the synthesis of the ϵ-phase ensures its epitaxial ϵ(100) || MgO(001) growth. At the temperature of the inverse martensitic transformation $A_S \sim 220$°C, the γ-phase appears from the ϵ-martensite through the martensitic mechanism. With a further increase in the annealing temperature above 600°C, the desorption of Mn atoms from the film begins. As a result, the chemical bonds of the Mn atoms with Fe atoms break and Mn atoms migrate from the γ-phase lattice. This gives rise to the instability of the γ-phase and its inverse transition to the stable α-Fe phase with the conservation of the initial Fe(001)[110] || MgO(001)[100] orientation relations. Similar phase transitions were revealed in epitaxial Mn/Si(111) films with an increase in the annealing temperature. The mixing of Mn with Si begins at about 100°C and finishes at about 400°C by the formation of the MnSi(111) phase through the

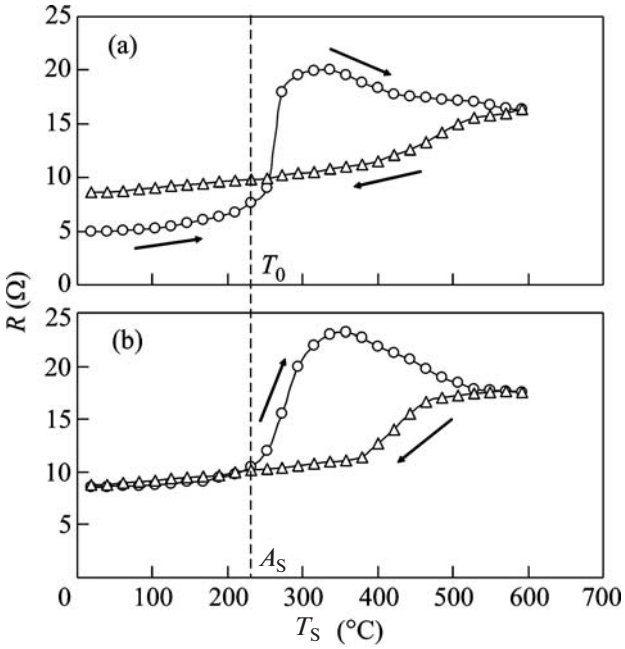

Fig. 4. Annealing temperature dependence of the electric resistance $R(T_S)$ of the Mn/Fe(001) film sample for two successive heating cycles up to 600°C. In the first cycle shown in panel (a), $R(T_S)$ increases sharply at the initiation temperature $T_0 \sim 220$°C of the solid-phase reaction between the Mn and Fe layers. In the second cycle shown in panel (b), similar changes in $R(T_S)$ occur at the temperature A_S of the inverse martensitic transformation, which coincides with the temperature T_0 ($T_0 = A_S \sim 220$°C).

solid-phase synthesis. The further heating above 600°C leads to the complete desorption of Mn from the MnSi(111) film [14].

Numerous investigations indicate that a unique feature of the solid-phase synthesis in thin films is that an increase in the annealing temperature is accompanied by the formation of only one (first) phase at the interface of film reagents at a certain temperature (initiation temperature T_0), although several phases are present in the phase diagram (see [15] and references therein). As shown in [16–20], the first phase appears at the minimum temperature T_K of a solid-phase structural transformation in a given binary system and the initiation temperature T_0 of the first phase coincides with the temperature T_K ($T_0 = T_K$). This first-phase rule is valid for many diffusion structure transformations [16]. The martensitic transformations belong to diffusion-free transformations. However, low-temperature solid-phase reactions in Ni/Ti, Au/Cd, and Al/Ni bilayer films start at the temperatures A_S of the inverse martensitic transformation in the NiTi ($A_S \sim 100$°C) [17, 18], AuCd ($A_S \sim 67$°C) [17, 19], and AlNi ($A_S \sim 220$°C) [17, 20] phases ($T_0 = A_S$), respectively. In all of the above systems, the B2 austenite phase first appears; it transforms to martensite phases below the temperature A_S. Under different cooling conditions, the reaction products can include both the austenite and martensite phases. The Fe–Mn phase diagram has no solid-phase transformations except for the $\epsilon \longleftrightarrow \gamma$ martensitic transformation. According to the above first-phase rule, atomic mixing at the Mn/Fe interface should start at the temperatures A_S of the inverse martensitic transformation and the reaction products should include both the ϵ-martensite and γ-austenite phases. Figure 4 shows the annealing temperature dependence of the electric resistance $R(T_S)$ of the Mn/Fe(001) samples after two successive heating cycles up to 600°C. In the first cycle, the sharp increase in the resistance at the temperature $T_0 \sim 220$°C is associated with the synthesis of the γ-phase, which has larger resistivity than the initial Mn/Fe(001) film (see Fig. 4a). The repeated heating of the sample is also accompanied by a sharp increase in the electric resistance at a temperature of about 220°C. However, the temperature ~220°C in this case is associated with the $\epsilon \longrightarrow \gamma$ martensitic transformation and is the temperature A_S of the inverse martensitic transformation. The experimental values of the synthesis initiation temperature T_0 and the temperature A_S of the inverse martensitic transformation coincide with each other ($T_0 = A_S \sim 220$°C). This result and the formation of the ϵ martensite phase in the samples after the reaction clearly indicate that the phase formation in Mn/Fe film structures follows the above first-phase rule. For this reason, we assume that the Mn–Fe phase diagram in the region of high iron contents includes a solid-phase transformation with a temperature of about 220°C. This conclusion is in good agreement with new thermodynamic calculations, which imply the existence of the solid-phase transformation with a temperature of about 200°C in the Mn–Fe phase diagram [21].

CONCLUSIONS

Phase transformations in epitaxial Mn/Fe(001) thin films with 24 at % of Mn have been analyzed with an increase of the annealing temperature up to 800°C. The formation of the ϵ martensite phase begins at a temperature of about 220°C at the Mn/Fe interface with the prevailing $\epsilon(100) \parallel MgO(001)$ orientation. An increase in the annealing temperature above 600°C leads to the desorption of Mn atoms from the $\epsilon(100)$ phase and the repeated formation of the epitaxial Fe(001) layer. The analysis of solid-phase reactions in thin films allows for the assumption that the solid-phase synthesis of the ϵ-phase is attributed to the $\epsilon \longrightarrow \gamma$ martensitic transformation in the Mn–Fe system. In this case, the temperature A_S of the inverse martensitic transformation coincides with the initiation temperature T_0 ($T_0 = A_S \sim 220$°C). According to the analysis of the solid-phase synthesis in Mn/Fe(001) thin films, a new low-temperature (~220°C) structural transfor-

mation assumingly exists in the Mn–Fe system with a high iron content.

This work was supported by the Russian Foundation for Basic Research (project no. 07-03-00190) and by the Ministry of Education and Science of the Russian Federation (project no. 2.1.1/4399, program "Development of the Scientific Potentiality of Higher Education" in 2009–2010).

REFERENCES

1. C. Demangeat and J. C. Parlebas, Rep. Prog. Phys. **65**, 1679 (2002).
2. S. K. Nayak and P. Jena, Chem. Phys. Lett. **289**, 473 (1998); S. Blügel, M. Weinert, and P. H. Dederichs, Phys. Rev. Lett. **60**, 1077 (1988).
3. X. Jin, Y. Chen, X. W. Lin, et al., Appl. Phys. Lett. **70**, 2455 (1997); B. Heinrich, A. S. Arrott, J. F. Cochran, et al., J. Vac. Sci. Technol. A **4**, 1376 (1986).
4. S. J. Lee, J. P. Goff, G. J. McIntyre, et al., Phys. Rev. Lett. **99**, 037204 (2007); T. K. Yamada, M. M. J. Bischoff, G. M. M. Heijnen, et al., Phys. Rev. Lett. **90**, 056803 (2003); S. Andrieu, M. Finazzi, Ph. Bauer, et al., Phys. Rev. B **57**, 1985 (1998).
5. E. C. Passamani, B. Croonenborghs, B. Degroote, et al., Phys. Rev. B **67**, 174424 (2003).
6. P. Torelli, F. Sirotti, and P. Ballone, Phys. Rev. B **68**, 205413 (2003).
7. Z. Zhou, Q. Li, and D. Venus, J. Appl. Phys. **99**, 08N504 (2006).
8. E. Carpene, F. Caccavale, L. M. Gratton, et al., Hyperfine Interact. **113**, 419 (1998).
9. M. Uhrmacher, A. Kulinska, Y. V. Baldokhin, et al., Hyperfine Interact. **136–137**, 327 (2001); V. V. Tcherdyntsev, S. D. Kaloshkin, et al., Z. Metallkd. **90**, 747 (1999).
10. A. T. W. Kempen, F. Sommer, and E. J. Mittemeijer, Acta Mater. **50**, 3545 (2002); X. Lu, Z. Qin, Y. Zhang, et al., Scripta Mater. **42**, 433 (2000); A. S. Hamada, P. Sahu, S. Ghosh Chowdhury, et al., Metall. Mater. Trans. A **39**, 462 (2008).
11. V. L. Sedov, *Antiferromagnetism of Gamma-Iron. The Invar Problem* (Nauka, Moscow, 1987) [in Russian].
12. C. Kim, J. H. Seo, and B. P. Rao, J. Appl. Phys. **102**, 113904 (2007); J. Seifert, T. Bernhard, M. Gruyters, and H. Winter, Phys. Rev. B **76**, 224405 (2007); L. Sun and H. Xing, J. Appl. Phys. **104**, 043904 (2008).
13. V. G. Myagkov, V. C. Zhigalov, L. E. Bykova, et al., J. Magn. Magn. Mater. **305**, 334 (2006); V. G. Myagkov, V. C. Zhigalov, L. E. Bykova, et al., J. Magn. Magn. Mater. **310**, 126 (2007).
14. H. Suto, K. Imai, S. Fujii, et al., Surf. Sci. **603**, 226 (2009).
15. E. G. Colgan, Mater. Sci. Rep. **5**, 1 (1990); R. Pretorius, C. C. Theron, A. Vantomme, and J. W. Mayer, Crit. Rev. Solid. State Mater. Sci. **24**, 1 (1999); T. Laurila and J. Molarius, Crit. Rev. Solid. State Mater. Sci. **28**, 185 (2003).
16. V. G. Myagkov, L. E. Bykova, and G. N. Bondarenko, Zh. Eksp. Teor. Fiz. **115**, 1756 (1999) [JETP **88**, 963 (1999)]; V. G. Myagkov, L. E. Bykova, V. S. Zhigalov, et al., Dokl. Akad. Nauk **371**, 763 (2000) [Dokl. Phys. **45**, 157 (2000)]; V. G. Myagkov, L. E. Bykova, V. S. Zhigalov, et al., Pis'ma Zh. Eksp. Teor. Fiz. **71**, 268 (2000) [JETP Lett. **71**, 183 (2000)]; V. G. Myagkov, L. E. Bykova, and G. N. Bondarenko, Dokl. Akad. Nauk **390**, 35 (2003) [Dokl. Phys. **48**, 30 (2003)]; V. G. Myagkov, L. E. Bykova, G. N. Bondarenko, et al., Pis'ma Zh. Eksp. Teor. Fiz. **88**, 592 (2008) [JETP Lett. **88**, 515 (2008)].
17. L. E. Bykova, V. G. Myagkov, and G. N. Bondarenko, Khim. Inter. Ustoich. Razv. **13**, 137 (2005).
18. V. G. Myagkov, L. E. Bykova, L. A. Li, et al., Dokl. Akad. Nauk **382**, 463 (2002) [Dokl. Phys. **47**, 95 (2002)].
19. V. G. Myagkov, L. E. Bykova, and G. N. Bondarenko, Dokl. Akad. Nauk **388**, 46 (2000) [Dokl. Phys. **45**, (2000)].
20. V. G. Myagkov, L. E. Bykova, S. M. Zharkov, et al., Solid State Phenom. **138**, 377 (2008).
21. V. T. Witusiewicz, F. Sommer, and E. J. Mittemeijer, J. Phase Equilib. **25**, 346 (2004).

Translated by R. Tyapaev